NUMERICAL ANALYSIS OF ELECTRON DISTRIBUTION FUNCTION UNDER ELECTRON CYCLOTRON HEATING DURING TOKAMAK START-UP

[1]N. TSUJII, A. EJIRI, K. SHINOHARA, Y. PENG, Y. LIN, Z. JIANG, Y. TIAN, F. ADACHI, Y. JIANG, S. WANG, M. YOSHIDA and Y. TAKECHI

[1]The University of Tokyo, Kashiwa, Japan

Email: tsujii@k.u-tokyo.ac.jp

We report our progress in the understanding of tokamak start-up assisted by electron cyclotron (EC) waves. The dynamics of collisionless electrons was studied using a numerical simulation based on the orbit-averaged kinetic theory. The impact of the relativistic effect was investigated and was found to be greater at stronger vertical field due to higher electron energy. The electron distribution function was predicted to have a characteristic shape regardless of the presence of the loop voltage because of the strong acceleration of electrons with turning point at the EC resonance. The finding was applied to extended MHD equilibrium reconstruction and evolution of the global electron distribution function during closed flux surface formation was obtained for the first time.

Large superconducting tokamaks have limited loop voltage that it is challenging to start-up a tokamak plasma reliably only with the central solenoid (CS). EC waves have been used successfully to assist start-up under such conditions [1]. Although application of EC waves to initiate breakdown under the conventional field-null configuration is beneficial, further improvement of the operational parameter space was found experimentally when the trapped particle configuration (TPC) was used [2]. It was found in the TST-2 spherical tokamak that higher plasma current can be reached with the same CS flux swing under the TPC compared to the conventional field-null configuration [3]. The improvement was especially large at low neutral pressure and high EC power. In contrast, the difference between the two configurations was negligible at high neutral pressure, which strongly suggested that collisionless electrons were responsible for the positive effects of the TPC.

A finite-element simulation based on the orbit-averaged kinetic theory was developed to study collisionless electron transport [4]. Figure 1(a,b) shows the result of the vertical field scan with and without the relativistic effect on TST-2. Overall, the mean energy scaled as the square of the vertical field strength whereas the plasma current scaled almost linearly. Relativistic effect reduced both mean energy E and plasma current I_p, but the ratio I_p/E, which can be considered a proxy of plasma current ramp rate per unit EC power, remained unchanged. The toroidal current density simulated with EC wave only and with both EC wave and loop voltage are shown in Fig. 1(c) and (d), respectively. Regardless of the presence of the loop voltage, a characteristic current distribution was predicted to the low-field side of the EC resonance due to strong acceleration of electrons with the turning point at the resonance.

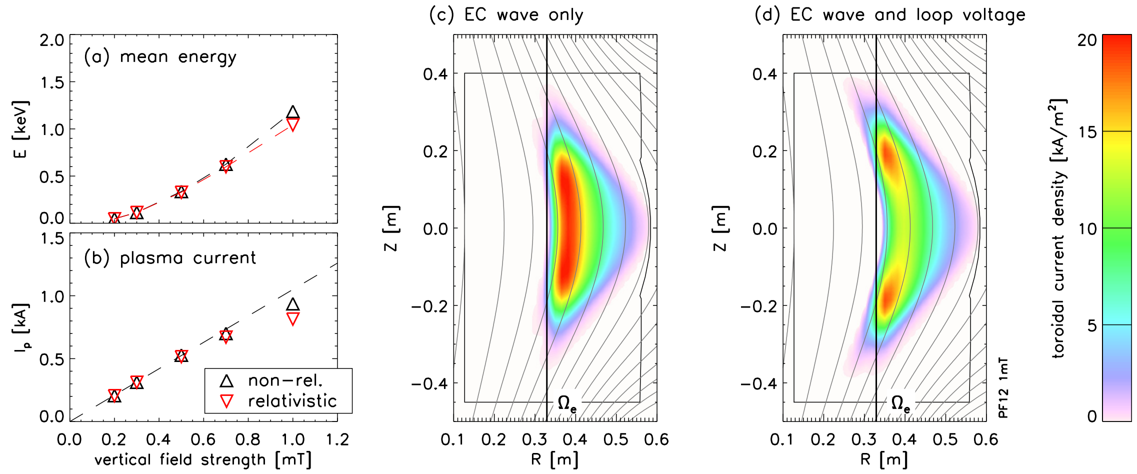

FIG. 1. The orbit-averaged kinetic simulation results on the TST-2 spherical tokamak. The vertical field dependence of the mean energy (a) and the plasma current (b) with and without the relativistic effect. Toroidal current density with EC wave only (c) and with EC wave and loop voltage of 0.5 V (d). The EC resonance radius (0.32 m) is shown with the vertical line. Gray solid curves: poloidal flux contours.

To estimate the time evolution of the electron distribution function, extended MHD equilibrium reconstruction [5] was applied to the EC assisted start-up experiment. The orbit-averaged electron distribution function was parametrized as follows:

$$f(E,\mu,P_\phi) = \exp\left(-E/T + (\mu/\mu_c - 1)/\delta_\mu\right)\cos\left((\pi/2)(P_\phi - P_0)/\delta P\right) \text{ if } \mu < \mu_c \text{ and } |P_\phi - P_0| < \delta P$$

and zero otherwise. E, μ and P_ϕ are the electron energy, magnetic moment and toroidal angular momentum, respectively. μ_c is the critical value of μ for reflection at the EC resonance and $\delta_\mu = 0.1$, P_0 and δP was set to cover the vertical column up to the limiter and $T = 0.1$ keV for the present analysis. The form captures the characteristic distribution shown in Fig. 1(c). We did not model the small loop voltage effect for this first attempt. Figure 2(a-d) shows the overview of the typical EC assisted Ohmic start-up discharge on TST-2. EC power was applied to initiate breakdown until burn through was reached as can be seen in the D_α trace (c). The results of the extended MHD equilibrium reconstruction are shown in Fig. 2(e,f). With extended MHD, the kinetic current carried by electrons with confined orbits can generate an equilibrium that fits the magnetic measurements even when the field lines are open. The evolution of the global electron distribution function was obtained for the first time seamlessly from just after breakdown (e) until closed flux surface formation (f).

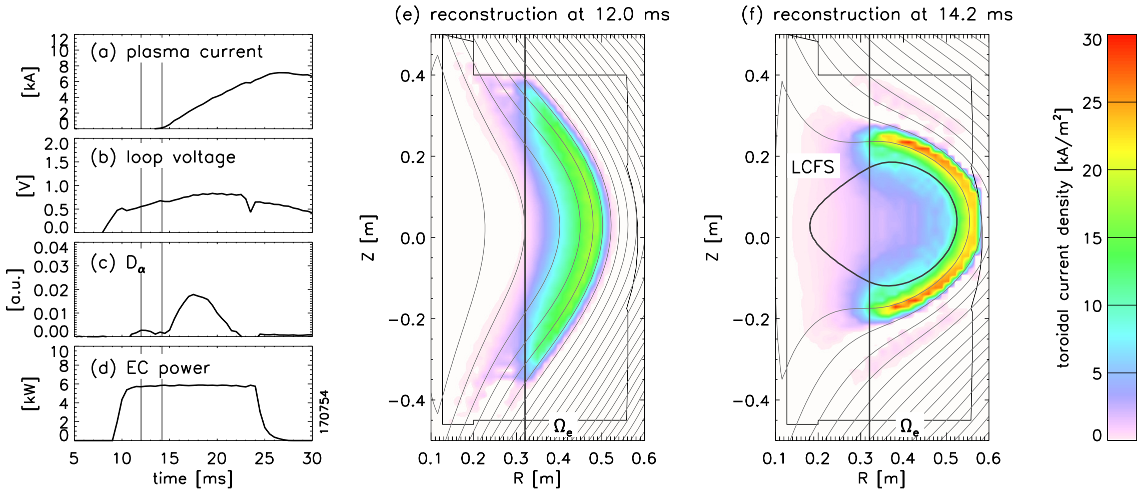

FIG. 2. (a-d) Overview of the time evolution of the EC wave assisted Ohmic start-up discharge on the TST-2 spherical tokamak. (a) Plasma current (b) loop voltage (c) D_α emission (d) O-mode fundamental EC power. The vertical lines are drawn at 12.0 ms and 14.2 ms. (e,f) The results of the extended MHD equilibrium reconstruction at 12.0 ms (e) and 14.2 ms (f). The EC resonance radius (0.32 m) is shown with the vertical line. Pseudo-color plot: toroidal current density. Gray solid curves: poloidal flux contours. The thick curve shows the last-closed flux surface (LCFS).

We have successfully applied the orbit-averaged kinetic simulation and the extended MHD equilibrium reconstruction to obtain the evolution of the global electron distribution function during the EC wave assisted Ohmic start-up phase. This information will allow us to understand the dynamics of collisionless electrons and their impact on plasma current evolution. Such an understanding is essential to fully predict and optimize EC assisted tokamak start-up that will likely be necessary for present and future large superconductive devices.

REFERENCES

[1] Wakatsuki, T., et al., Achievement of the first tokamak plasma with low inductive electric field in JT-60SA, Nucl. Fusion **64** (2024) 104003.

[2] An, Y., et al., Efficient ECH-assisted plasma start-up using trapped particle configuration in the versatile experiment spherical torus, Nucl. Fusion **57** (2016) 016001.

[3] Ko, Y., Tsujii, N., et al., Optimization of Poloidal Field Configuration for Electron Cyclotron Wave Assisted Low Voltage Ohmic Start-Up in TST-2, Plasma Fus. Res. **16** (2021) 1402056.

[4] Tsujii, N., et al., Kinetic Analysis of the Characteristics of Electron Cyclotron Heating Assisted Ohmic Start-Up in the Trapped Particle Configuration of a Tokamak, Plasma Fus. Res. **18** (2023) 1402051.

[5] Tsujii, N., et al., Modification of the magneto-hydrodynamic equilibrium by the lower-hybrid wave driven fast electrons on the TST-2 spherical tokamak, Nucl. Fusion **61** (2021) 116047.